Anti-inflammatory Effects of Hydrogen in LPS-induced RAW264.7 Cells via Inhibiting NF-κB and MAPKs Signaling Pathways

Tao Zhang
Chongqing University of Technology
Fuping Wang
Chongqing University of Technology
Guoqiang Jiang
Yishengrui (Shanghai) Biotechnology Co., Ltd
Guobao Chen
Chongqing University of Technology
Lili Han
Chongqing University of Technology
Zhongmin Chen (chenzhongmin@cqut.edu.cn)
Chongqing University of Technology

Research Article

Keywords: Hydrogen, Anti-inflammatory property, NF-κB pathway, MAPKs pathway, RNA sequencing

Posted Date: November 12th, 2021

DOI: https://doi.org/10.21203/rs.3.rs-1035921/v1

Abstract

Hydrogen (H_2), a new type of medical gas molecule, which has significant preventive effect on numerous diseases and its anti-inflammatory properties has been proven in previous studies. However, the mechanisms of H_2 anti-inflammatory activity in signal transduction pathway or protein level regulation are inadequately inexplicit. In the current study, the effect of H_2 on LPS-induced inflammation in RAW 264.7 cells were assessed and its molecular mechanisms were clarified. The in vitro model of inflammation was induced by lipopolysaccharide (LPS) in RAW264.7 cells. Cell viability was evaluated by MTT assay. Protein expression of inflammatory mediators were analyzed by ELISA and Western blot. mRNA levels were detected by RT-qPCR. In addition, RNA sequencing (RNA-seq) was conducted to explore the molecular targets of H_2 anti-inflammatory. According to the findings, H_2 reversed LPS-induced variety in NO levels and TNF-a production as well as IL-6, IL-10 proteins and related mRNA levels in macrophages. RNA-seq newly discovered that H_2 acted on inflammatory signaling molecule protein kinase C 8 (PKC8) and heterodimer activator protein-1 (AP-1). The WB analysis was then used to determine the key proteins in the inflammatory signaling pathway involved in PKC8 and AP-1, which found that H_2 inhibited the phosphorylation of key proteins in the NF-kB and MAPKs pathways, thereby the expression of mRNA and inflammatory mediators were affected. The findings of this study show that H_2 may serve as a promising anti-inflammatory gas in mitigating inflammatory conditions.

Introduction

Inflammation acts as the body's first response following the entrance of external pathogens through the human barrier. It is a non-specific immune response and occur in all tissues and organs of the body [1], which external manifestations are comprised of redness, swelling, heat, pain, and dysfunction. Inflammation responses is triggered when immune cells recognize pathogen-associated molecular patterns (PAMPs) [2]. Inflammation is one of the body's defense mechanisms against external invasions and is often beneficial. However, the impact of inflammation on the body should be considered in two aspects [3]. Specifically, excessive accumulation of pro-inflammatory cytokines and mediators may cause changes in the structure of tissues and organs, which in turn affects normal function even leads to serious diseases, such as cancer and cardiovascular diseases [4]. Therefore, it is necessary to control the inflammatory responses process and minimize the adverse effects of inflammation on the human body.

Macrophages are distributed in various tissues of the human body and play an important role in the elimination of pathogens, inflammatory responses, and repairing tissue damage. A variety of Toll-like receptors (TLR) are expressed on the surface of macrophages [5]. TLR4 is an important TLR, which could be activated by a variety of PAMPs [6]. The high expression of TLR4 receptor on macrophages enables macrophages to quickly activate and plays a role in response to pathogen invasion [7]. LPS is a component of the cell wall in Gram-negative bacteria, which is recognized by the TLR4 receptor on the surface of macrophages [8]. After TLR4 is activated, it dimerizes and changes its intracellular conformation. The downstream adapters recruited by TLR4 include MyD88, TIRAP, TRIF, TRAM and

SARM [9]. Among them, MyD88 acts as an adaptor protein in most TLR signaling pathways, which can be recruited through its N-terminal death domain (DD) and activated downstream kinases containing the same domain, such as IRAK4 and IRAK2. It can further activate TRAF6 and downstream TAK1 as well as IkBa and MAPKs subsequently [10]. Thus, the signal transduction pathways of NF-kB and MAPKs transcription are activated, and the transcription of related inflammatory factors are initiated [11-13]. In recent years, the emergence of a substantial amount of novel anti-inflammatory drug has effectively controlled the inflammatory reaction process. Yang et al. found that the methylation inhibitor 3-Deazaadenosine inhibited AP-1 and NF-kB by blocking MEK1/2 and IKKa/b or indirectly mediating SAHH, resulting in the production of anti-inflammatory activity [8]. Li et al. found that Gegen Qinlian decoction, a traditional Chinese medicine decoction, could inhibit TLR4/NF-kB signal transduction and play a role in the treatment of ulcerative colitis [14]. In addition, Xie et al. found that Magnesium Isoglycyrrhizinate extracted from licorice inhibits the translocation of NF-kB as well as the activation of MAPKs by inhibiting IKK phosphorylation and IkB-a degradation, thereby inhibiting the inflammatory response [15]. Although these anti-inflammatory drugs have a clear mechanism of action and satisfactory results against inflammation, they have problems such as high preparation cost and long treatment cycles. As a new type of gas with anti-inflammatory effects, H_2 has been confirmed to regulate inflammation signal pathways, which has attracted close attention from the medical community [16].

Under normal temperature and pressure, the binding force of H_2 and hemoglobin is much less than that of O_2. Therefore, it is considered a physiologically inert gas. In 2007, Ohsawa et al. proposed that H_2 could selectively scavenge oxygen free radicals, exert anti-inflammatory and antioxidant functions, and it has been confirmed that hydrogen could improve cerebral ischemia-reperfusion injury in an animal model, which has attracted widespread attention [17]. Researchers at home and abroad have also demonstrated that H_2 has good antioxidant and anti-inflammatory activities through a variety of animal experiments [18,19]. Previous studies have shown that hydrogen-rich water can improve various inflammatory symptoms such as colitis, hepatitis, and pancreatitis [20-22]. Moreover, various studies have suggested that the anti-inflammatory effect of H_2 is related to the reduction of oxidative stress injury and is involved in the regulation of signal transduction pathways such as P38-MAPK and NF-kB [23, 24]. Although the research in this area continues to make progress, the signal transduction pathway of the hydrogen molecule's anti-inflammatory properties or the regulation mechanism of protein levels are poorly understood.

H_2 has been shown to alleviate inflammation and oxidative stress both in vivo or in vitro conditions [25, 26]. Therefore, in this study, the cytotoxicity and anti-inflammatory effects of H_2 on RAW264.7 cells as well as the cytokines levels and NO secretion were assayed. Meanwhile, RNA-seq was applied to conduct enrichment analysis of the differential expression on inflammatory genes. Finally, the specific mechanisms that H_2 effected macrophages were studied and the differential expression of related signal proteins in the TLRs-mediated pathway was demonstrated.

Materials And Methods

Materials

RAW264.7 cell, Dulbecco's modified Eagle's (DMEM), NO reagent kit was acquired from Beyotime Institute of Biotechnology (Shanghai, China). FDA and PI were purchased from sigma-Aldrich (St. Louis, MO, USA) Lipopolysaccharides (LPS, from Escherichia coli O55:B5), Fetal bovine serum (FBS), Phosphate buffered saline (PBS) were acquired from Beijing Solarbio Science & technology Co., Ltd. (Beijing, China). The inflammatory mediators (TNF-a, IL-6, IL-10) ELISA kits were obtained from MEI-MIAN (Shanghai, China). Primary antibodies against p65, P-IκBa, IkBa, P-JNK, JNK, P-ERK, ERK, P-P38, P38, iNOS, c-Fos, c-Jun, b-Actin, Lamin B1 were purchased from Cell Signaling Technology (Danvers, MA, US). All other chemicals and reagents used were of analytical grade.

Hydrogen health machine (YSR-600B) and portable dissolved hydrogen analyzer were provided by Yishengrui (Shanghai) Biotechnology Co., Ltd. (Shanghai, China).

Cell culture and preparation of hydrogen-contain medium

RAW264.7 cells were cultured in DMEM supplemented with 10% FBS at 37 ℃ in a humidified incubator with 5% CO_2, for which the medium was changed every other day. For subcultures, cell growth density was approximately 80% for passage, with seeds at a dilution of 1:3. Cells in the logarithmic growth phase were used in this experiment.

Under normal environment, the hydrogen health machine was used to pass H_2 into DMEM. H_2 concentration in the medium was then measured with a portable dissolved hydrogen analyzer. The introduction of H_2 was stopped when the concentration reached 1.2 ppm. During cell culturing, the H_2 was kept in the medium at a concentration of 1.2 ppm.

MTT assay

Cell viability was determined using the MTT assay. Briefly, RAW264.7 cells (5×10^3 cell/well) were seeded in 96-well plates and were then cultivated for 24 h. After treating cells with H_2 (1.2 ppm) for 12 h, they were incubated with or without of LPS (1 mg/mL) for 12 h. Then, MTT solution (100 mL, 0.5 mg/mL) was added to each well and incubated at 37 ℃ for 4 h. The medium was discarded and 100 mL DMSO was added to dissolve the formazan crystals. The absorbance value was measured at 490 nm using a microplate reader. Three parallel experiments were performed for each group.

FDA/PI staining assay

The cells were stained with FDA/PI to qualitatively evaluate the effects of H_2 and LPS on cell viability. Here, 1 mL of PBS was added into 1 mL of FDA staining solution (5 mg/mL, soluble in acetone solution) and PI staining solution (5 mg/mL, soluble in PBS solution). After staining for 5 min in the dark, the staining solution was discarded washed twice with PBS which was then observed under a fluorescence microscope.

NO, TNF-a, IL-6, and IL-10 determination

RAW264.7 cells were then seeded in a 24-well plate at 1×10^5 cells/mL. After 6 h, RAW264.7 cells were cultured in medium with or without H_2 for 12 h, which were then stimulated with or without 1 mg/mL LPS for 24 h. The supernatant was collected at different time points (0, 3 h, 6 h, 12 h, and 24 h). The Griess method was used to determine the effect of H_2 on NO secretion of LPS-stimulated macrophages. The contents of TNF-a, IL-6, IL-10 in the supernatant were determined according to the instructions of the ELISA kit.

Measurement of iNOS activity

RAW264.7 cells (1×10^5 cells per well in 24-well plates) were treated with 1 mg/mL LPS for 12 h. After being washed thrice by PBS, the cells were incubated in present or absence of H_2 (1.2 ppm) for a further 12 h. The supernatants were collected, and the level of NO production was monitored by measuring the nitrite level in the culture medium using Griess method. The relative iNOS activity was calculated by normalizing to NO levels of the Con group [27].

RNA extraction and RT-qPCR

RAW264.7 cells were treated with H_2 (1.2 ppm) for 12 h prior to the stimulation with LPS (1 mg/mL) for 24 h. For determining the relative gene expression of iNOS, TNF-a, IL-6, IL-10. The primers used in this assay are listed in Table. 1. Total RNA was isolated from cells using Trizol reagents according to the manufacturer's instructions (Beyotime Biotechnology, China). The quality and quantity of RNA were determined by measuring the absorbance at 260 nm and 280 nm using a microplate reader. The obtained RNA was reverse-transcribed by M-MuLV First Strand cDNA Synthesis Kit (Sangon, China) according to the manufacturer's instructions. The qPCR analysis was conducted on a BIOER Fluorescent Quantitative Detection System (Bioer Technology, China) using the respective primers and KAPA SYBR® FAST Universal 2X qPCR Master Mix (Roche, Switzerland). The transcript levels (fold changes) of target mRNAs were normalized to b-actin and were quantified using the $2^{-\Delta\Delta Ct}$ method [28].

cDNA library construction

The cDNA library was constructed using the TruSeq^{TM} RNA sample preparation kit (Illumina, San Diego, CA, USA) according to the manufacturer's instructions. First, the total RNA was segmented by magnetic beads, then Super Script double-stranded cDNA synthesis kit (Invitrogen, CA, USA) was used to add six base random primers (Illumia). The first cDNA was retro-transcribed with mRNA as the template, after which double-stranded synthesis was carried out to form a stable structure. End Repair Mix was added to repair the end of the segment and a base was added to the 3'END to connect the Y-shaped joint. The purified products were enriched over 15 cycles to create a cDNA library.

Gene expression analysis

Gene expression analysis was performed in accordance with the procedure [29]. First, FASTX-Toolkit-0.0.13.2 (http://hannonlab.cshl.edu/fastx_toolkit) was used to examine the quality of raw reads generated by HisSeq 2000, including base sequence content and quality, pre-base distribution of mean error. The Trimmomatic software (version 0.35) was used to remove low-quality bases and adapter sequences. Then, RNA sequence quality control software package (RSeQC-2.3.2) (http://code.google com/p/rseqc/) was used to comprehensively evaluate RNA-seq data, including reads repeatability, error rate and coverage uniformity.

Bowtie 2 software was used to compare clean reads with reference genomes in orientation mode. Calculate the expression level of each transcript. Then, using the fragments per kilobase of exon per million mapped reads (FRKM) to identify differential expression genes from two sample. After running TopHat, the comparison file obtained was provided to Cuffdiff (http://cufflinks.cbcb.umd.edu/) for differential expression analysis.

The Omicshare (http://www.omicshare.com/) was used to draw heatmap. Gene ontology (GO) function enrichment and Kyoto Encyclopedia of Genes and Genomes (KEGG) pathway analysis were carried out by DAVID (http://david.ncifcrf.gov) and KOBAS v2.0 (http://kobas.cbi.pku.edu.cn/home.do) to query the functions of the differentially expressed genes.

Protein isolation and western blot analysis

RAW264.7 cells were plated in a 25 cm^2 cell culture flask (2×10^6 cells/mL) and were incubated for 6 h. They were then cultured with or without H_2 for 12 h and stimulated by LPS with or without 1mg/mL for 24 h. The cells were then washed and collected with ice-cold PBS to extract the intracellular protein. Used the kit (Solarbio Science & technology Co., Ltd, China) by the centrifugal method (12000g/min, 15min each time) to extract total cell protein, cytoplasmic protein and nuclear protein, respectively. The concentration of extracted protein was determined using the BCA method (Beyotime Biotechnology, China). The denatured protein was added in equal amount (30 mg per sample) to 12% SDS-PAGE gel, after which they were transferred to the PVDF membranes. After blocking with 5% skim milk (dissolved in 0.1% tween 20 TBST), the PVDF membrane was incubated with primary antibodies at 4 ℃ overnight. The primary antibodies were collected, and the secondary antibody conjugated with peroxidase was incubated at room temperature for 1 h. The bound antibody was detected using the enhanced chemiluminescence (ECL) detection system (Bio-rad, USA), and data was quantified using Image J software (Stuttgart, Germany) [30].

Statistical analysis

Results were expressed as means ± standard deviations (SDs) based on data obtained from three independent experiments. A student's t-test was used to determine the significant difference between stimulation group and control group. When more than two groups compared, One-way analysis of variance (ANOVA) with Tukey's HSD test was carried out assess the significance of the difference by the SPSS (version 20.0). The differences were considered as statistically significant when $p< 0.05$.

Results

Effect of H_2 on viability of RAW264.7 cells

In order to eliminate the false positives of inhibitory cytokines due to their non-specific cytotoxicity, the safe doses of H_2 and LPS were initially evaluated. Before investigating the H_2 anti-inflammatory mechanism, MTT and FDA/PI staining assay were used to determine cell viability following treatment with H_2 (1.2 ppm) and LPS (1 mg/mL) for 24 h. As shown in Fig. 1A-B, H_2 (1.2 ppm) and LPS (1 mg/mL) did not show significant cytotoxicity within the set concentrations. Therefore, subsequent experiments were carried out under these conditions.

Effect of H_2 on the expression of NO, TNF-a, IL-6 and IL-10 in LPS-induced RAW264.7 cells

In order to examine the effect of H_2 on the inflammatory response mediated by macrophages, RAW264.7 cells were pre-incubated with H_2 (1.2 ppm) for 12 h, and then stimulated with LPS for 24 h, the cytokines and chemokine productions of cells at different time points were analyzed by ELISA (Fig. 2A-D). Compared with the control group, the levels of NO, TNF-a, IL-6, and IL-10 were all found to be significantly increased after LPS stimulated, while NO, TNF-a, and IL-6 reached peak values at 6 h (13.57, 11.76 and 9.35-folds) and IL-10 at 24 h was 11.19 times that of the control group. However, in the H_2 treatment group, the levels of NO, TNF-a, and IL-6 decreased (p <0.05), while the level of IL-10 increased (p <0.05). The inhibitory effect of H_2 on NO, TNF-a, IL-6 reached 31.41%, 32.73% and 38.35% at 6 h, and the promotion of IL-10 at 24 h reached 37.68%.

Effect of H_2 on iNOS activity in LPS-induced RAW 264.7 cells

LPS stimulation for 12 h would induce macrophages to generate iNOS, while after removing LPS, there would be no stimulation to macrophages and no increase of iNOS generation. Given that, the treatment with H_2 to macrophages would pose no impact on the iNOS content in cell and only potentially suppress the activity of the iNOS generated. However, there is no fall of NO content in supernatant after H_2 addition, H_2 is thus of no direct scavenging effects on the generated NO and no obvious suppression on the iNOS activity in further conclusion (Fig. 3A).

H_2 inhibited protein expression of iNOS in LPS-induced RAW264.7 cells

In macrophages, NO is mainly produced by inducible nitric oxide synthase (iNOS). Therefore, the alteration of iNOS protein expression following H_2 treatment was further examined. As shown in Fig. 3B, iNOS protein level was significantly increased after LPS treatment (p < 0.01), while it was significantly inhibited in the H_2 treatment group. Compared with the LPS group, the inhibition rate of iNOS in the H_2 treatment group was 28.57%, which was consistent with the corresponding decrease in NO content. The results showed that H_2 inhibited the release of NO by inhibiting the expression of iNOS protein in RAW264.7 cells induced by LPS.

Effect of H_2 on the iNOS, TNF-a, IL-6 and IL-10 mRNA of LPS-induced RAW264.7 cells

The effect of H_2 on the expression of NO, TNF-a, IL-6, and IL-10 mRNA were investigated by RT-qPCR. As shown in Fig. 4, compared with the control group, LPS treatment was shown to significantly ($p < 0.01$) increase the mRNA levels of NO, TNF-a, IL-6, and IL-10. However, it was observed that H_2 had a significant inhibitory effect on the expression levels of NO, TNF-a and IL-6 by 30.37%, 31.61% and 20.90%, respectively. In addition, H_2 was found to significantly promote mRNA expression level of IL-10 (29.96%). The changes in NO, TNF-a, IL-6, and IL-10 mRNA were consistent with the corresponding cytokines, which confirmed that the anti-inflammatory effect of H_2 occurs at the transcriptional level.

Sequence analysis

As shown in Table. 2. In culture conditions containing LPS, 49243916, 52103720 and 53628676 reads were acquired in the LPS group, while 54937040, 45621726, and 51051502 reads were acquired in the LPS/H_2 group. After accusation and deletion of low-quality sequences, the LPS group had 48936036, 51763020, 53223022 reads, while the LPS/H_2 group had 54490962, 45310890, 50704868 reads. The error rates of both groups were less than 0.1%, with a GC percentage of around 50%, indicating that the gene distribution was uniform. More than 90% of the two sets of groups possessed a base quality of 20%, while about 90% of the two sets of groups reached a basic quality value of 30%.

The content of the repeated reads in each group were found to be within the normal range, with no obvious peaks at both ends of the abscissa of all samples, indicating the great uniformity of each sequence. Most genes with medium or above expression levels (i.e., genes with quantitative values >3.5) were close to saturation in comparing 40% of the sequenced reads (the ordinate value approaches 1), indicating that the overall quality of saturation was high. In general, the RNA-Seq data was of high quality and could be analyzed later.

Difference analysis of gene expression

The difference of gene expression between the LPS group and LPS/H_2 group were analyzed. Compared with the LPS group, the H_2 treatment group was shown to significantly regulate 323 genes, of which 167 genes were significantly down-regulated ($p < 0.05$) and 156 genes were significantly up-regulated ($p < 0.05$) (Fig. 5A and 5C). The differential expression pattern is shown in Fig. 5B. In the heat map, different reads represent the expression values of different genes, which are distinguished by different colors (Fig. 5D). As the expression value changed from high to low, the color changed from red to blue. It also shows that there are differences in the expression of 323 genes between the LPS group and the LPS/H_2 group.

Biological processes and Immune-related pathways

Cluster analysis was performed for genes with significant differential expression by GO enrichment and KEGG enrichment. The GO classification system describes the attributes of cell genes and gene products according to three aspects: Biological Process (BP), Cellular Component (CC), and Molecular Function

(MF). BP classification mainly includes cellular processes and cellular regulation. CC classification relates to cell phase and cell partial stage, while MF classification includes a binding provision (Fig. 5E). Our experiment studied the inflammatory regulation effect of H_2 on LPS-induced RAW264.7 cells, so the focus is on BP classification, especially in multi-biological and multi-cellular biological processes.

GO enrichment analysis can reflect the degree of influence of the experiment design on each classification to a certain extent. However, the mechanism behind these biological functions should be understood. Pathway analysis can provide a more comprehensive and systematic understanding of the biological processes of cells. KEGG is a database that is commonly used in signaling pathway research. As shown in Fig. 5F, through a KEGG enrichment analysis, a total of 88 genes/transcripts related to the immune system were found to be affected by H_2, which were distributed in the two major metabolic pathways of Organismal Systems (77) and Human Disease (11). Among them, the specific pathway was found to be Th17 cell differentiation (Pathway ID: map 04659) with up to 20 genes/transcripts, followed by Th1 and Th2 cell differentiation (Pathway ID: map 04658) with 13, IL-17 signaling pathway (pathway ID: map 04657) with 5. By analyzing these signal pathways, it was found that H_2 affects the inflammatory response of RAW264.7 cells and is related to the NF-kB and MAPKs signaling pathways. As shown in Fig. 6, the regulation of the NF-kB signaling pathway was related to the inhibition of the upstream linker signal PKC8; meanwhile, H_2 in the MAPKs pathway was noted to affect transcription activator AP-1, which has not been reported in previous studies. H_2 eventually affected the secretion of related inflammatory factors through the regulation of signal proteins.

Western blot verification of NF-kB and MAPKs pathways

According to the RNA-Seq results, H_2 was shown to exert anti-inflammatory effects by inhibiting the activation of upstream signaling molecules (PKC8) and transcriptional activator (AP-1), thereby inhibiting the activation of the NF-kB and MAPKs signaling pathways. However, previous studies have shown that H_2 treatment inhibited the phosphorylation of extracellular kinase (ERK), c-jun N-terminal kinase (JNK) and P38 MAPK, and NF-kB p65 activation [31]. Therefore, other inflammation-related important signaling molecules in these two signaling pathways were investigated, which further demonstrated the results of the KEGG enrichment analysis and previous research results. Activated by upstream kinases, IkBa is rapidly phosphorylated and degraded to release inhibition of the NF-kB p50 and p65 subunits. Therefore, the level of phosphorylation and degradation of IkBa after LPS stimulation, as well as the translocation of NF-kB p65 subunit from cytoplasm to nucleus, can be used to represent the activation degree of the NF-kB signaling pathway [45]. As shown in Fig. 7A, P-IkBa levels in RAW264.7 macrophages were found to be significantly increased following LPS stimulation, indicating that LPS stimulation led to rapid phosphorylation and degradation of IkBa. However, H_2 was observed to significantly inhibit this process, indicating that the anti-inflammatory effect of H_2 is related to the phosphorylation regulation of key proteins in the NF-kB signaling pathway. Therefore, in order to further demonstrate that H_2 acts on the NF-kB pathway, the expression of p65 in cell was measured. It was found that the protein levels of p65

subunit significantly decreased in the cytoplasm and increased in the nucleus following LPS stimulation, indicating that the p65 subunit migrated from the cytoplasm to the nucleus. However, H_2 was shown to have obvious inhibitory effect on this process. Fig. 7B showed that after LPS stimulated the phosphorylation levels of ERK, P38, and JNK increased by about 3.48, 1.10, and 3.30-fold, respectively, while the inhibition rates of ERK, P38, and JNK phosphorylation levels in the H_2 treatment group were 16.67%, 23.00%, and 73.30%, respectively. The results of WB demonstrated that in the NF-kB pathway, H_2 not only acts on the PKC8 signaling molecule, but also has a significant inhibitory effect on the phosphorylation of IkBa and the nuclear translocation of p65; In the MAPKs pathway, H_2 treatment inhibited the phosphorylation of ERK, JNK and P38 MAPK, and our results prove the reliability of RNA-Seq results and previous research results.

Effect of H_2 on LPS-induced AP-1 activity by MAPKs signaling pathway.

AP-1 is controlled by MAPKs, including ERK1/2, JNK/SAPK and P38 MAPK. Following detection of these three proteins and their phosphorylation, AP-1 activity was assessed, which included c-Jun and c-Fos. The results demonstrated that AP-1 activity in RAW264.7 macrophages induced by LPS was significantly increased ($p < 0.05$), while H_2 significantly inhibited ($p < 0.01$) AP-1 (c-Jun and c-Fos) activity. The inhibition rate of c-Jun was 80.86% while the inhibition rate of c-Fos was 27.20% (Fig. 7C). These findings further demonstrate the results of RNA-Seq.

Discussion

Macrophages are the most powerful phagocytes in the body; their phagocytic and immune signal transduction functions play important roles in the body's specific and non-specific immunity [32]. There are multiple of Toll-like receptors (TLRs) on the surface of macrophages, which recognize components of pathogens and activate for phagocytosis as well as the release of inflammation-related mediators [33]. However excessive secretion of inflammatory factors will aggravate the inflammatory response, ultimately causing damage to the tissues and macrophages themselves. As a widely distributed gas in nature, H_2 has been proven to confer protection against ischemia/reperfusion injury of multiple organs, respiratory disease, and neurodegenerative diseases [34]. However, the research on the molecular mechanism of H_2 is still incomplete. Therefore, the anti-inflammatory properties and molecular targets of H_2 were investigated at the molecular level in this study.

LPS is an endotoxin with certain cytotoxicity. It is unclear whether H_2 has potential side effects. Therefore, whether H_2 and LPS inhibit the release of inflammatory factors from macrophages by affecting cell viability should be ruled out. Before investigating the anti-inflammatory mechanism of H_2, the toxicity of H_2 (1.2 ppm) and LPS (1 mg/mL) were determined using the MTT assay. The experimental results showed that RAW264.7 cells did not decrease in cell proliferation activity under the set levels of H_2 and LPS, which was also demonstrated by FDA/PI staining. Therefore, in the subsequent experiments, a concentration of 1.2 ppm of H_2 and 1 mg/mL of LPS were used. NO is an inflammatory mediator

secreted by macrophages, which produced is catalyzed by nitric oxide synthase (iNOS) [35] using L-arginine as a substrate and consumes O_2. In addition to NO, macrophages can also release other inflammatory factors, such as TNF-a, IL-6 and IL-10 after being stimulated by LPS. In addition to self-regulating inflammation, TNF-a also stimulates the other cytokines through paracrine or autocrine effects on the TNF receptor (TNFR) [36]. IL-6 is another inflammatory factor secreted by macrophages, which can induce the differentiation and maturation of immune effector cells such as monocytes and B cells and play a role in inflammation and fever [37]. IL-10 is an anti-inflammatory factor that inhibits the expression of inflammatory factors TNF-a and IL-6 through activated macrophages [38]. Excessive production of pro-inflammatory mediators, including NO, TNF-a, IL-6 or insufficient production of anti-inflammatory factors like IL-10, leads to a disturbance in the internal environment, which is an important contributor in the development of inflammation. In this study, the intervention effect of H_2 on inflammation was investigated in the LPS-induced RAW264.7 cell inflammation model. The results demonstrated that the inhibition of NO, TNF-a, and IL-6 secretions in the LPS-induced RAW264.7 cells reached a peaked at 6 h ($p < 0.01$). However, the secretions of IL-10 continued to rise within 24 h over time. While, H_2 has a regulatory effect on the abnormal secretion of inflammatory mediators. Research on the inhibitory effect of H_2 on NO demonstrated that its inhibitory effect stems from the inhibition of iNOS protein expression levels (the inhibition rate was 28.57%), rather than directly inhibiting the enzyme activity of iNOS or directly scavenging the generated NO free radicals. Therefore, since H_2 is a gas with anti-inflammatory activity, it may be able to regulate the secretion of cytokines, which is consistent with previous studies [39]. In order to confirm whether H_2 regulates the expression of these proteins by affecting its transcription level, RT-qPCR method was used to determine the effects of H_2 on the mRNA expression levels of iNOS, TNF-a, IL-6, and IL-10 in LPS-induced cells. The results showed that H_2 could inhibit the mRNA levels of iNOS, TNF-a and IL-6 in RAW264.7 cells induced by LPS while increasing IL-10 mRNA level.

In view of the difference in the expression of inflammatory factors related to mRNA in RT-qPCR, the LPS group and LPS/H_2 group were selected and the Illumina RNA-Seq method was used to explore the signal transduction pathways and molecular targets of H_2. In this study, the expression levels of the 88 genes exhibited significant differences following H_2 treatment. According to the GO and KEGG databases, the annotation analysis of differentially expressed genes revealed that H_2 was mainly involved in influencing the NF-kB and MAPKs signaling pathways. Previous studies have found that hydrogen-rich water inhibits inflammation and apoptosis through the JNK and P38-MAPK signaling pathways, thereby reducing the symptoms of acute liver injury associated with acute necrotizing pancreatitis in SD rats [21]. Li et al. gave hydrogen-rich water to rats with global cerebral ischemia-reperfusion injury via intraperitoneal injection and found that H_2 could reverse the up-regulation of NF-kB and TNF-a expression, down-regulate TGF-b1 expression, and decrease the number of regulatory T lymphocytes [40]. A recent study showed that hydrogen/oxygen mixed gas inhalation improves disease severity and dyspnea in patients with coronavirus disease 2019 (COVID-19) [41]. These findings indicate that H_2 may be considered potential therapeutic molecules for the treatment of inflammatory disease. However, in this study, the anti-

inflammatory effect of H_2 was found to be related to the inhibition of PKC8 and AP-1 activation, which has not been reported previously. PCK8 is a member of the PKC family. As a multifunctional kinase, PKC plays an important role in gene expression and regulation [42]. The activation of PKC can lead to the high expression of NF-kB, which in turn causes inflammation, while H_2 inhibits the activation of the NF-kB signaling pathway by inhibiting the activation of PKC8. AP-1 is one of the most critical transcription factors for cell growth and differentiation, which is regulated by activated MAPKs in the inflammatory response. The activated MAPKs phosphorylate the Ets transcripts, initiate the transcription of Fos gene, and express c-Fos protein and c-Jun protein to form the AP-1 complex [43]. The two transcription factors PKC8 and AP-1 have a synergistic effect, which initiate gene transcription and ultimately synthesizes inflammation-related proteins. The results of the KEGG analysis demonstrate that H_2 also has a significant inhibitory effect on the activation of AP-1.

The TLR4 receptor on the surface of macrophages can recognize LPS and activate two inflammatory signaling pathways: NF-kB and MAPKs. However, previous studies have shown that H_2 treatment inhibited the phosphorylation of ERK, JNK and P38 MAPK, and NF-kB p65 activation [31]. Therefore, we verified the previous studies through WB experiments. In the NF-kB signaling pathway, IkBa is phosphorylated and rapidly ubiquitinated and then degraded, thereby releasing the inhibition of IkBa on p50 and p65 in the NF-kB signaling pathway. The NF-kB p65 subunit translocases to the nucleus and binds to the promoter to activate the expression of target genes [44]. In this study, H_2 was shown to significantly inhibit ($p < 0.01$) the phosphorylation of IkBa and p65 following 24 h of treatment, indicating that H_2 plays a negative regulatory role in the activation of the NF-kB signaling pathway induced by LPS. Unlike NF-kB, AP-1 is controlled by MAPKs, including ERK1/2, JNK/SARK, and P38-MAPK. Studies have shown that the ERK, JNK, and P38 kinase cascade pathways are independent and interact with each other, and eventually activate the heterodimer AP-1 composed of c-Jun and c-Fos, which enters the nucleus and initiates the transcription of related inflammatory factors [45]. The experimental results showed that H_2 inhibited LPS-induced phosphorylation of ERK, JNK and P38, and AP-1 activation. Western blot analysis demonstrated the results of the RNA-Seq enrichment analysis and previous studies, and further clarified the molecular mechanism of H_2's anti-inflammatory properties.

Conclusions

This study performed to clarify the anti-inflammatory mechanism of H_2. The results demonstrated that at a concentration of 1.2 ppm, H_2 showed significant anti-inflammatory activity on LPS-induced RAW264.7 cells within 24 h, which was achieved by inhibiting the activation of NF-kB and MAPKs signaling pathways. Specifically, RNA-seq and WB results showed that H_2 acts on the PKC8 signaling molecule and heterodimer AP-1, and at the same time exerts an anti-inflammatory effect by inhibiting the phosphorylation of other signaling proteins in the signaling pathway. Its inflammation regulation process is shown in Fig. 8. The findings of this study show that H_2 and hydrogen-rich production may serve as a potential alternative approach to the management and prevention of inflammation or related diseases. However, there are still some problems remain to be solved, such as determining the optimal method,

amount, and frequency of H_2 administration for each human disease. Furthermore, H_2 is a flammable and explosive gas. How to control its concentration and prevent gas leakage requires in-depth consideration.

Declarations

Acknowledgements

This research was supported by the Chongqing Technology Innovation and Application Development Project (cstc2019jscx-msxmX0110).

Competing Interests

The authors have declared no competing financial interest.

Author Contribution

Zhongmin Chen and Tao Zhang together conceived the study, participated in its design and coordination, and drafted the manuscript. Tao Zhang was mainly in charge of the protein assay and inflammatory mediators' analysis. Fuping Wang and Guobao Chen planned experiments and guided experiments. Guoqiang Jiang provided experimental equipment. Lili Han performed experiments. All authors have read and approved the final manuscript.

References

1. Mankhong, S. *et al*. 4-methoxycinnamyl p-coumarate isolated from Etlingera pavieana rhizomes inhibits inflammatory response via suppression of NF-κB, Akt and AP-1 signaling in LPS-stimulated RAW 264.7 macrophages. *Phytomedicine* **54**, 89-97 (2019).

2. Mogensen, T.H. Pathogen recognition and inflammatory signaling in innate immune defenses. *Clin Microbiol Rev* **22** (2), 240-273 (2009).

3. Moreira, C.G. *et al*. Virulence and stress-related periplasmic protein (VisP) in bacterial/host associations. *Proc Natl Acad Sci USA* **110** (4), 1470-1475 (2013).

4. Xu. M, T.Y. *et al*. Yan-Hou-Qing formula attenuates ammonia-induced acute pharyngitis in rats via inhibition of NF-κB and COX-2. *BMC Complement Med Ther*. **20** (1), 280 (2020).

5. Lz, A. *et al*. Immunomodulatory activity of polysaccharide from Arca granosa Linnaeus via TLR4/MyD88/NFκB and TLR4/TRIF signaling pathways. *J Funct Foods* **84** (2021).

6. Gupta, P.K. *et al*. Activation of murine macrophages by G1-4A, a polysaccharide from Tinospora cordifolia, in TLR4/MyD88 dependent manner. *Int Immunopharmacol* **50**,168-177 (2017).

7. Gioannini, T.L. *et al*. Regulation of interactions of Gram-negative bacterial endotoxins with mammalian cells. *Immunol Res* **39** (1-3), 249-260 (2007).

8. Yang, W.S. *et al*. 3-Deazaadenosine, an S-adenosylhomocysteine hydrolase inhibitor, attenuates lipopolysaccharide-induced inflammatory responses via inhibition of AP-1 and NF-kappaB signaling. *Biochem Pharmacol* **182**, 114264 (2020).

9. O'Neill, L.A. *et al*. The family of five: TIR-domain-containing adaptors in Toll-like receptor signalling. *Nat Rev Immunol* **7** (5), 353-364 (2007).

10. Lye, E. *et al*. The role of interleukin 1 receptor-associated kinase-4 (IRAK-4) kinase activity in IRAK-4-mediated signaling. *J Biol Chem* **279** (39), 40653-40658 (2004).

11. Lomaga, A. *et al*. TRAF6 deficiency results in osteopetrosis and defective interleukin-1, CD40, and LPS signaling. *Genes Dev* **13** (8), 1015-1024 (1999).

12. Gohda, J. *et al*. Cutting edge: TNFR-associated factor (TRAF) 6 is essential for MyD88-dependent pathway but not toll/IL-1 receptor domain-containing adaptor-inducing IFN-beta (TRIF)-dependent pathway in TLR signaling. *J Immunol* **173** (5), 2913-2917 (2004).

13. Sato, S. *et al*. Essential function for the kinase TAK1 in innate and adaptive immune responses. *Nat Immunol* **6** (11), 1087-1095 (2005).

14. Li, R. *et al*. Gegen Qinlian decoction alleviates experimental colitis via suppressing TLR4/NF-kappaB signaling and enhancing antioxidant effect. *Phytomedicine* **23** (10), 1012-1020 (2016).

15. Xie, C. *et al*. Magnesium isoglycyrrhizinate suppresses LPS-induced inflammation and oxidative stress through inhibiting NF-kappaB and MAPK pathways in RAW264.7 cells. *Bioorg Med Chem* **27** (3), 516-524 (2018).

16. Yao, L. *et al*, Hydrogen-rich saline alleviates inflammation and apoptosis in myocardial I/R injury via PINK-mediated autophagy. *I Int J Mol Med* **44** (3), 1048–1062 (2019).

17. Ohsawa, I. *et al*. Hydrogen acts as a therapeutic antioxidant by selectively reducing cytotoxic oxygen radicals. *Nat Med* **13** (6), 688-694 (2007).

18. Tan , X. *et al*. The role of hydrogen in Alzheimer's disease. *Med Gas Res* **8** (4), 176-180 (2018).

19. Uto, K. *et al*. Hydrogen-rich solution attenuates cold ischemia-reperfusion injury in rat liver transplantation. *BMC Gastroenterol* **19** (1), 25 (2019).

20. Chen, X. *et al*. Lactulose mediates suppression of dextran sodium sulfate-induced colon inflammation by increasing hydrogen production. *Dig Dis Sci* **58** (6), 1560-1568 (2013).

21. Shi, Q. *et al*. Hydrogen-Rich Saline Attenuates Acute Hepatic Injury in Acute Necrotizing Pancreatitis by Inhibiting Inflammation and Apoptosis, Involving JNK and p38 Mitogen-Activated Protein Kinase-dependent Reactive Oxygen Species. *Pancreas* **45** (10), 1424-1431 (2016).

22. Chen, H. *et al*. Hydrogen-rich saline ameliorates the severity of l-arginine-induced acute pancreatitis in rats. *Biochem Biophys Res Commun* **393** (2), 308-313 (2010).

23. Zhang, Y. *et al*. Saturated hydrogen saline attenuates endotoxin-induced lung dysfunction. *J Surg Res* **198** (1), 41-49 (2015).

24. Liu, H. *et al*. Combination therapy with nitric oxide and molecular hydrogen in a murine model of acute lung injury. *Shock* **43** (5), 504-511 (2015).

25. Ren, J. D. *et al*. Hydrogen-rich saline inhibits NLRP3 inflammasome activation and attenuates experimental acute pancreatitis in mice. *Mediators Inflamm* **2014**, 930894 (2014).

26. Huang, P. *et al*. Hydrogen gas inhalation enhances alveolar macrophage phagocytosis in an ovalbumin-induced asthma model. *Int Immunopharmacol* **74**, 105646 (2019).

27. Han, Y. *et al*. Isodeoxyelephantopin, a sesquiterpene lactone from Elephantopus scaber Linn., inhibits pro-inflammatory mediators' production through both NF-κB and AP-1 pathways in LPS-activated macrophages. *Int Immunopharmacol* **84**, 106528 (2020).

28. Feng, M. *et al*. Anti-inflammatory effects of three selenium-enriched brown rice protein hydrolysates in LPS-induced RAW264.7 macrophages via NF-κB/MAPKs signaling pathways. *J Funct Foods* **76**, 104320 (2021).

29. Xia, B. *et al*. Gene expression profiling analysis of the effects of low-intensity pulsed ultrasound on induced pluripotent stem cell-derived neural crest stem cells. *Biotechnol Appl Biochem* **64** (6), 927-937 (2017).

30. Ren, B. *et al*. Ginsenoside Rg3 attenuates angiotensin II-induced myocardial hypertrophy through repressing NLRP3 inflammasome and oxidative stress via modulating SIRT1/NF-kappaB pathway. *Int Immunopharmacol* **98**, 107841 (2021).

31. Han, B. *et al*. MAPKs and Hsc70 are critical to the protective effect of molecular hydrogen during the early phase of acute pancreatitis. *FEBS J* **283** (4), 738-756 (2016).

32. Zhou, D. *et al*. Macrophage polarization and function with emphasis on the evolving roles of coordinated regulation of cellular signaling pathways. *Cell Signal* **26** (2) 192-197 (2014).

33. Lee, H. H. *et al*. Anti-inflammatory potential of Patrineolignan B isolated from Patrinia scabra in LPS-stimulated macrophages via inhibition of NF-κB, AP-1, and JAK/STAT pathways. *Int Immunopharmacol* **86**, 106726 (2020).

34. Ohno, k. *et al*. Molecular hydrogen as an emerging therapeutic medical gas for neurodegenerative and other diseases. *Oxid Med Cell Longev* **2012**, 353152 (2012).

35. Mankhong, S. *et al*. 4-methoxycinnamyl p-coumarate isolated from Etlingera pavieana rhizomes inhibits inflammatory response via suppression of NF-κB, Akt and AP-1 signaling in LPS-stimulated RAW 264.7 macrophages. *Phytomedicine* **54**, 89-97 (2018).

36. Zakharova, M. *et al*. Paradoxical Anti-Inflammatory Actions of TNF-α: Inhibition of IL-12 and IL-23 via TNF Receptor 1 in Macrophages and Dendritic Cells. *J Immunol* **175** (8), 5024-5033 (2005).

37. Stein, B. *et al*. IL-6 as a drug discovery target. Drug Discov Today **3** (5), 202-213 (1998).

38. Wen, C. *et al*. Regulation of Il-10 gene expression by Il-6 via Stat3 in grass carp head kidney leucocytes. *Gene* **741**, 144579 (2020).

39. Ying, Y. et al. Protective effect of hydrogen-saturated saline on acute lung injury induced by oleic acid in rats. *J Orthop Surg Res* **12** (1), 134 (2017).

40. Li, Q. *et al*. Neuroprotective Effect of Hydrogen-Rich Saline in Global Cerebral Ischemia/Reperfusion Rats: Up-Regulated Tregs and Down-Regulated miR-21, miR-210 and NF-κB Expression. *Neurochem Res* **41** (10), 2655-2665 (2016).

41. Guan, W. J. *et al*. Hydrogen/oxygen mixed gas inhalation improves disease severity and dyspnea in patients with Coronavirus disease 2019 in a recent multicenter, open-label clinical trial. *J Thorac Dis* **12** (6) 3448-3452 (2020).

42. Li, X. *et al*. Regulation of lipid metabolism in diabetic rats by Arctium lappa L. polysaccharide through the PKC/NF-kappaB pathway. *Int J Biol Macromol* **136**, 115-122 (2019).

43. Treisman, R. Regulation of transcription by MAP kinase cascades. *Curr Opin Cell Biol* **8** (2), 205-215 (1996).

44. Pham, T.H. *et al*. Fargesin exerts anti-inflammatory effects in THP-1 monocytes by suppressing PKC-dependent AP-1 and NF-κB signaling. *Phytomedicine* **24**, 96-103 (2017).

45. Kaminska, B. MAPK signalling pathways as molecular targets for anti-inflammatory therapy from molecular mechanisms to therapeutic benefits. *Biochim Biophys Acta* **1754** (1-2), 253-262 (2005).

Tables

Table. 1. Gene primers of inflammatory factor

	Forward	Reverse
iNOS	5'-CCTCACGCTTGGGTCTTGTT-3'	5’-GTGGACGGGTCGATGTCAC-3’
TNF-a	5’- TGTCTACTCCTCAGAGCCCC-3’	5’- TGAGTCCTTGATGGTGGTGC-3’
IL-6	5’-CTGCAAGAGACTTCCATCCAG-3’	5’-TTGGGAGTGGTATCCTCTGTGAAG-3
IL-10	5’-GACTTTAAGGGTTACCTGGGTTG-3’	5’-TCACATGCGCCTTGATGTCTG-3’
b-actin	5’-ATCACTATTGGCAACGAGCG-3’	5’-TCAGCAATGCCTGGGTACAT-3’

Table. 2. Summary statistics of sequencing data and sequencing quality control assessments for the data

Group	Sample	Raw reads	Clean reads	Error rate (%)	Q20 (%)	Q30 (%)	QG content (%)
LPS	B_1	54937040	54490962	0.0242	98.37	94.97	52.35
	B_2	45621726	45310890	0.0243	98.33	94.84	52.21
	B_3	51051502	50704868	0.0242	98.37	94.89	52.69
LPS/H_2	A_1	49243916	48936036	0.0239	98.5	95.26	52.52
	A_2	52103720	51763020	0.0241	98.4	95.01	52.44
	A_3	53628676	53223022	0.024	98.46	95.16	52.65

Figures

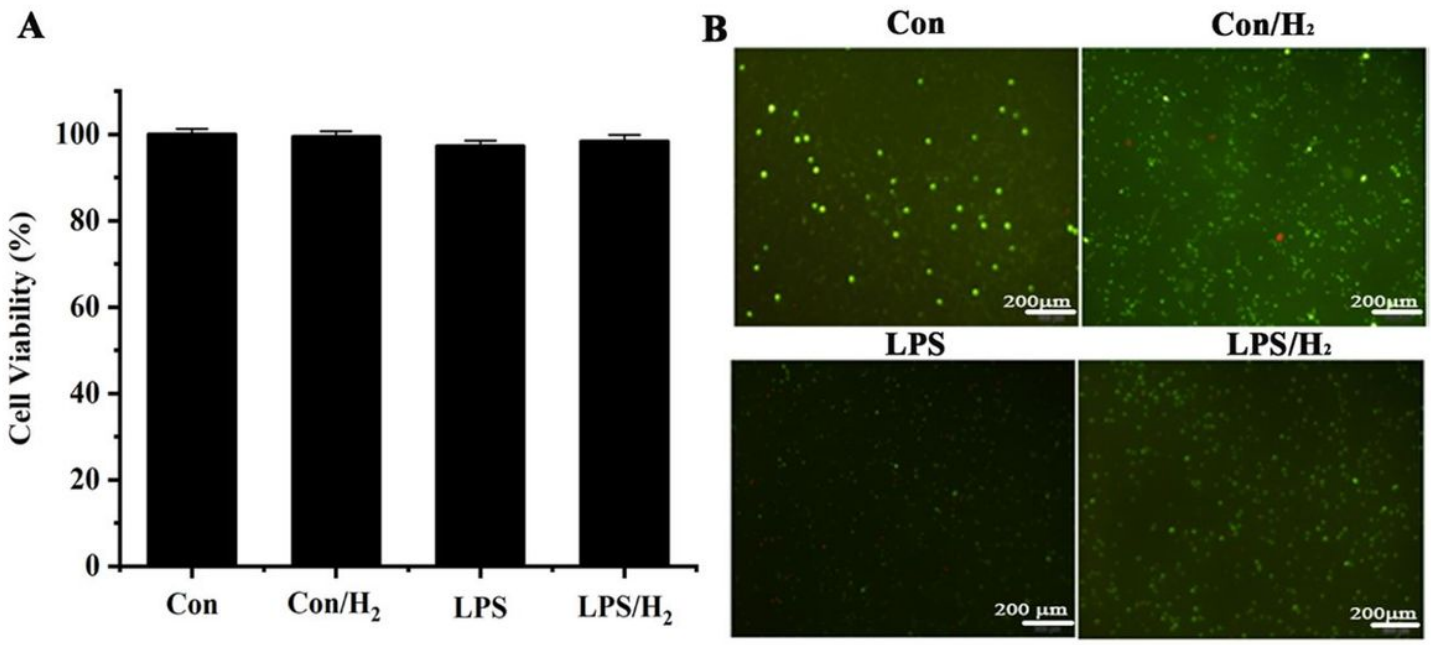

Figure 1

Effect of H2 and LPS on the viability of RAW264.7 cells. Cells were pre-treated with 1.2 ppm H2 for 12 h, and then stimulated with or without LPS for 24 h. The results are expressed as the mean ± SD (n=3); # $p < 0.01$ versus control group; * indicated $p < 0.05$, ** indicated $p < 0.01$ versus the LPS group. (A: cell viability determined by MTT; B: FDA/PI staining result)

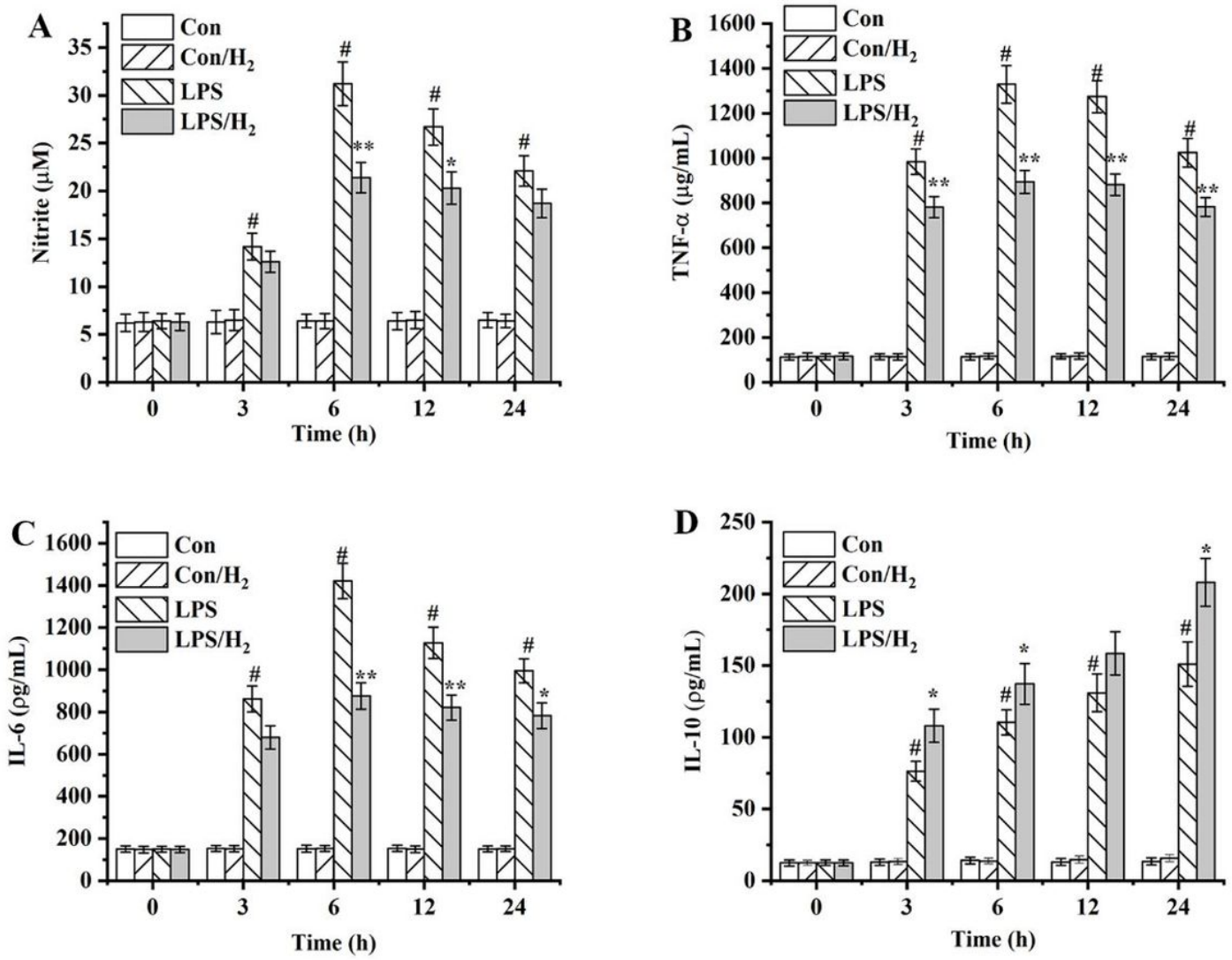

Figure 2

Effect of H2 on the production of NO (A), TNF-α (B), IL-6 (C), and IL-10 (D) in LPS-induced RAW264.7 cells. Cells were pre-incubated with or without 1.2 ppm H2 for 12 h, followed by stimulation with or without 1 μg/mL LPS for 24 h. The supernatant was collected then TNF-α, IL-6, and IL-10 were analyzed by ELISA. Nitrite levels in the culture medium were measured by Griess reaction. The results are expressed as the mean ± SD (n=3); # $p < 0.01$ versus control group; * indicated $p < 0.05$, ** indicated $p < 0.01$ versus the LPS group.

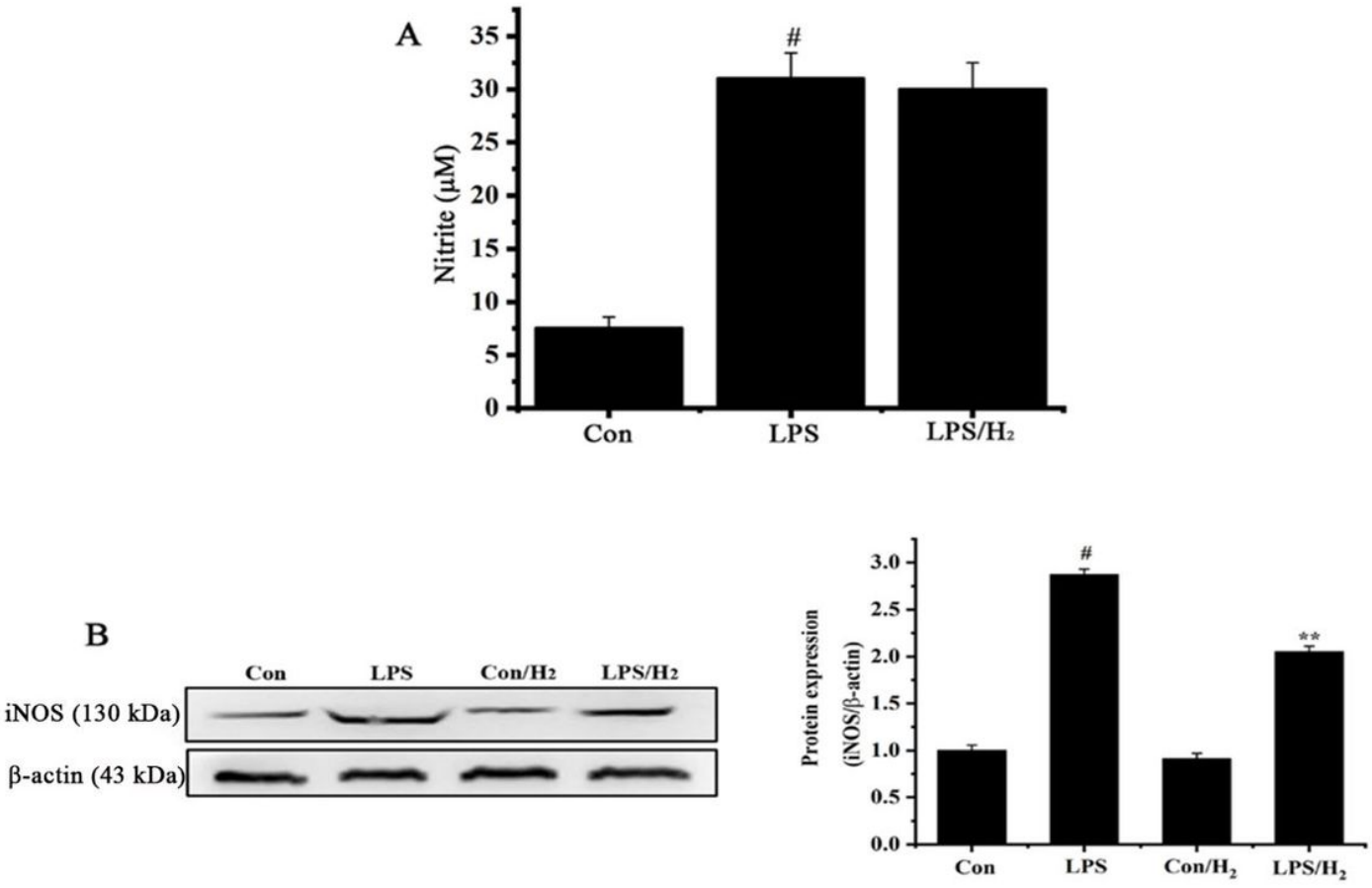

Figure 3

Effect of H2 on iNOS activity and protein expression. (A) Cells were pretreated with LPS (1 μg/mL) for 12 h, LPS was removed by washing, and the cells were treated with H2 (1.2 ppm) for an additional 12 h. Nitrite levels in the culture medium were measured. # $p < 0.01$ versus control group. (B) Representative western blotting images of iNOS protein. (The blots cropped from different parts of the same gel, and the gel was trimmed when the membrane was transferred. All blots are not processed for high-contrast.). The results are expressed as the mean ± SD (n=3); # $p < 0.01$ versus control group; * indicated $p < 0.05$, ** indicated $p < 0.01$ versus the LPS group.

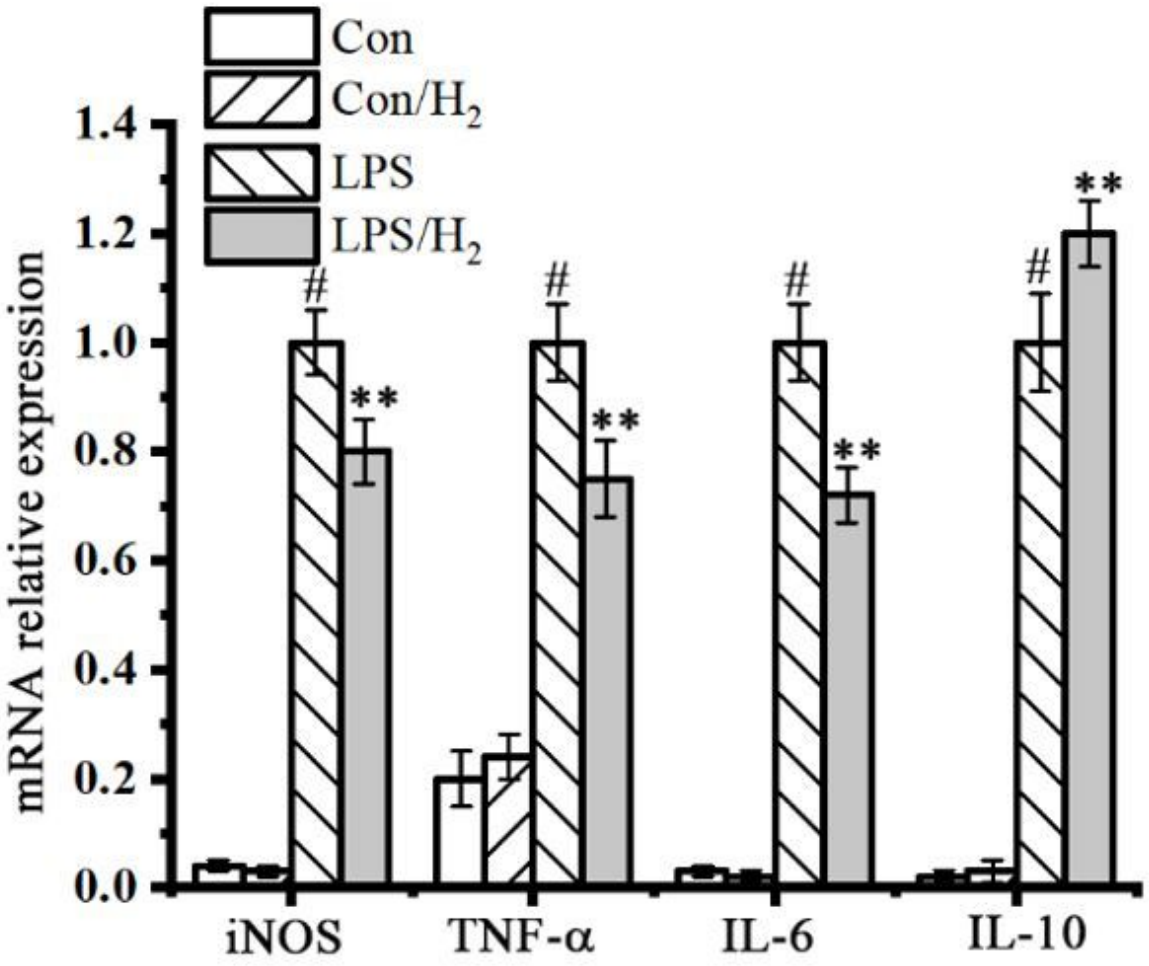

Figure 4

Effect of H2 on the mRNA expression of iNOS, TNF-α, IL-6, and IL-10 in LPS-induced RAW264.7 cells. Cells were pre-incubated with H2 for 12 h, followed by stimulation with LPS for 12 h. The mRNA expression of iNOS, TNF-α, IL-6 and IL-10 was determined by qPCR analysis. The results are expressed as the mean ± SD (n=3); # $p < 0.01$ versus control group; * indicated $p < 0.05$, ** indicated $p < 0.01$ versus the LPS group.

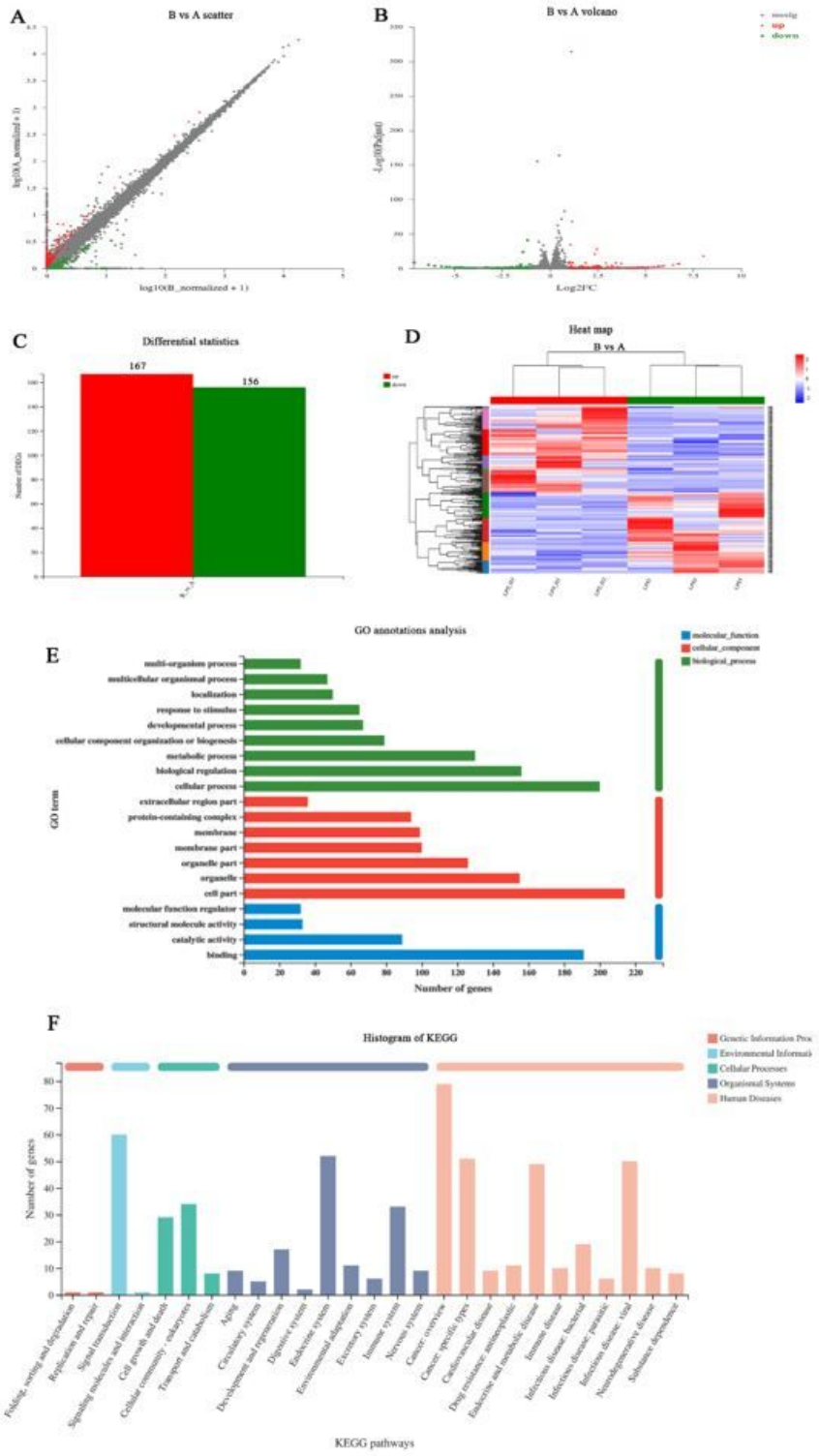

Figure 5

Summary statistics of differentially expressed genes and characterized the effect of LPS and H2 treatment on the expression of cell signaling molecules. (A) scatter plot of differentially expressed genes, (B) volcano plot of differentially expressed genes, each point represents a specific gene, in which green dots means a significant decrease of genes, red dots means a significant increase, and black dots mean insignificant genes; (C) bar graph of the number of significantly differentially expressed genes in LPS

group and LPS/H2 group, red color represent the number of high expression genes and green color represent the number of low expression genes; (D) heat map of the differentially expressed genes in the LPS group and LPS/H2 group each row represents a gene, and each column represents a sample, the color represent the expressive quantity of gene, in which red color represents the high expressive genes and green color represents the low expressive genes, right and top, clustering of genes and sample, represent; (E) GO classification of genes on the molecular function, cellular component and biological process levels in LPS group and LPS/H2 group, the horizontal axis gives the number of genes annotation to a GO term, the ordinate gives each detailed classification of GO; (F) KEGG enrichment of genes on genetic information process, environment information processing, cellular processes, organismal systems and human disease in LPS group and LPS/H2 group, the horizonal axis labels the secondary classification of KEGG terms, the left ordinate give the KEGG enrichment number.

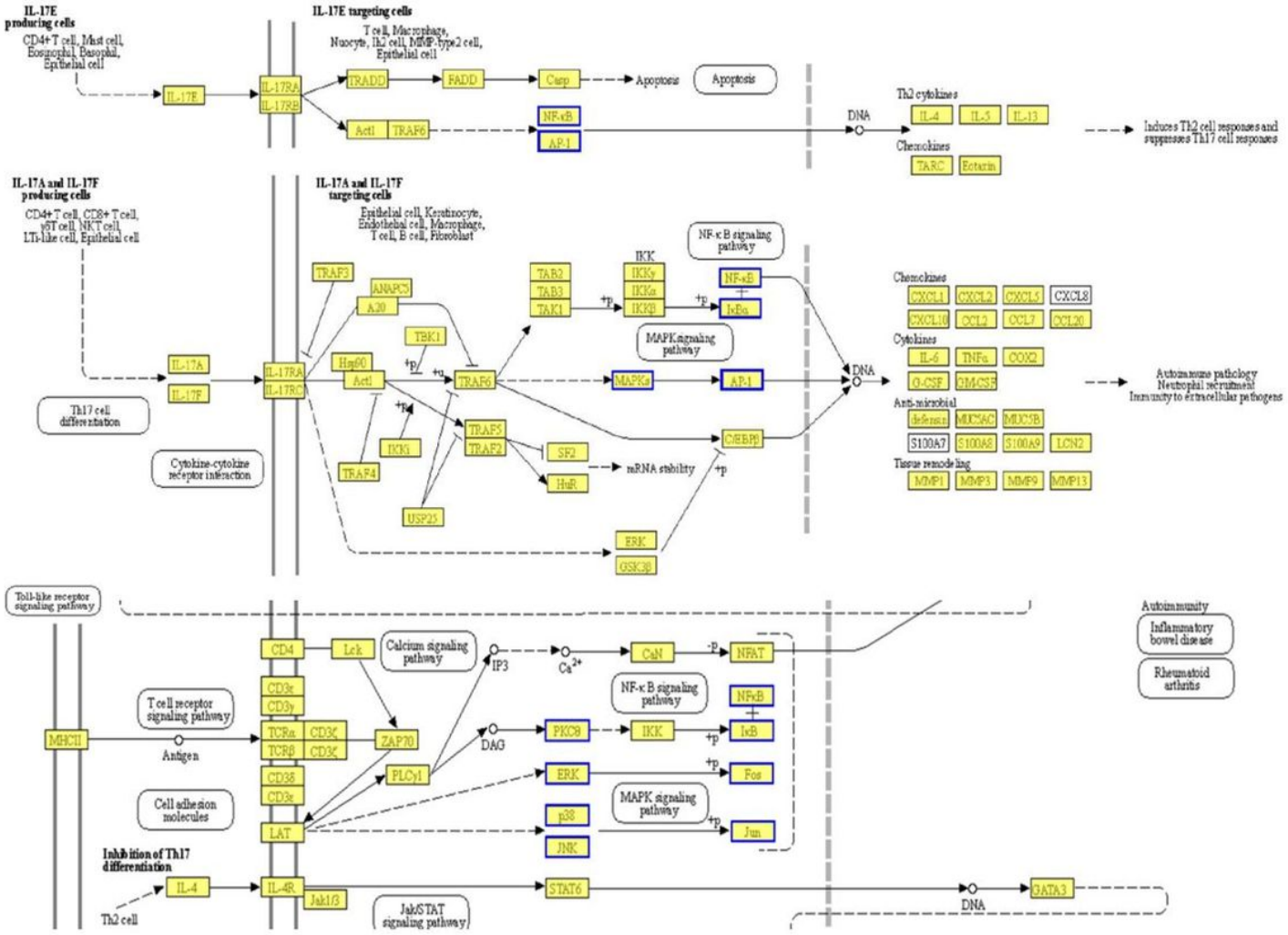

Figure 6

The molecular targets of H2 in NF-κB and MAPKs signaling pathways. NF-κB and MAPKs regulates genes played important roles in inflammation, immunity and cell survival. (Among them, H2 acts on PKC8 and AP-1, which are newly discovered in this research.)

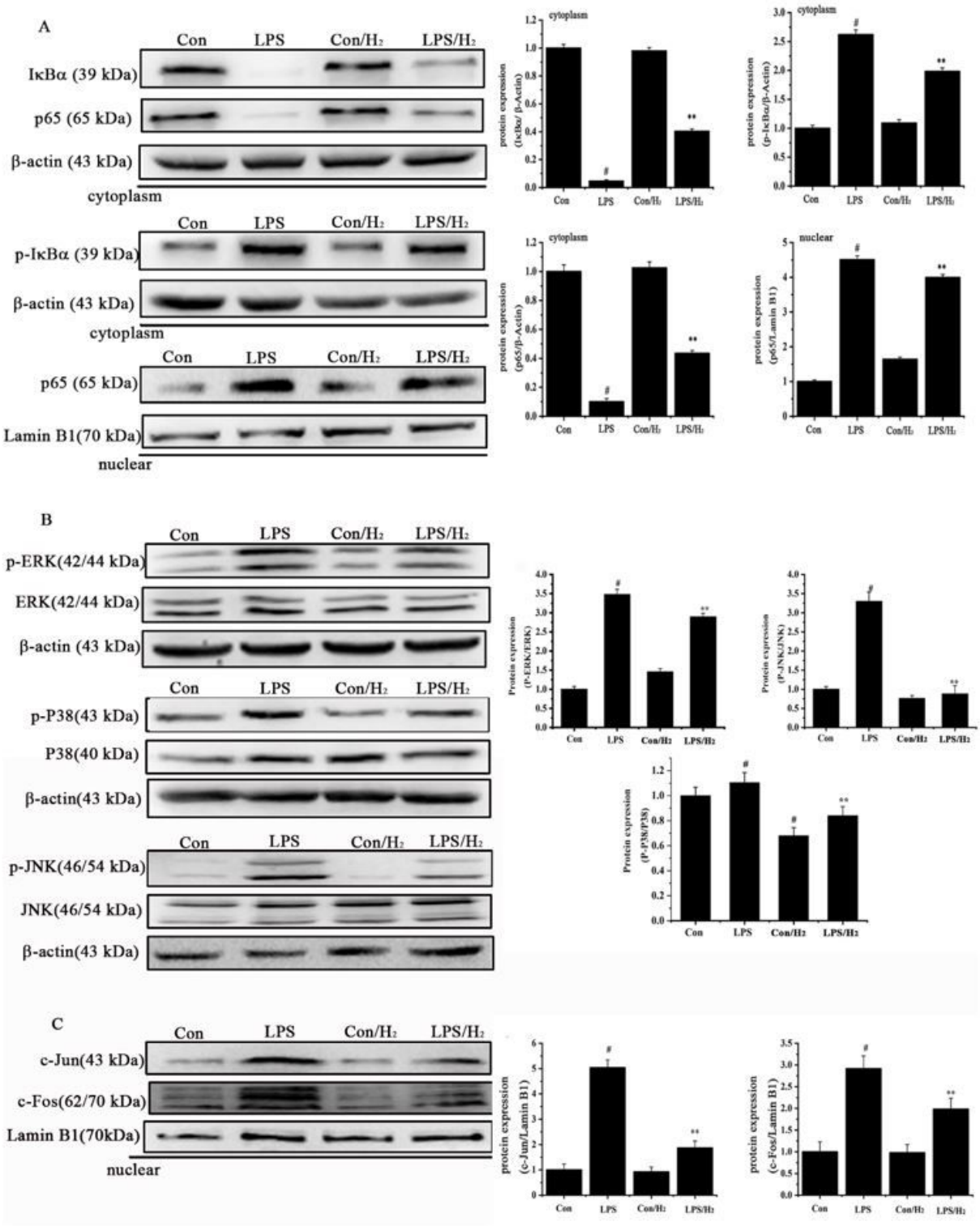

Figure 7

Effect of H2 on NF-κB and MAPKs signal pathways in LPS-induced RAW264.7 cells. All blots are not processed for high-contrast (overexposure). (A) Representative protein blots of p65 in nuclear and cytoplasm. The proteins expression of IκBα, P-IκBα, p65 in cytoplasm. The levels of p65 protein in nuclear. (The cytoplasm/nucleus western blot was derived from different parts of the same gel, and the gel was trimmed when the membrane was transferred.); (B) Representative western blotting images of

protein on MAPKs pathway in whole cell. (Blots are from different gels.) (C) Representative western blotting images of c-Jun and c-Fos in nucleus (Blots are from different gels.). The results are expressed as the mean ± SD (n=3); # $p < 0.01$ versus control group; * indicated $p < 0.05$, ** indicated $p < 0.01$ versus the LPS group.

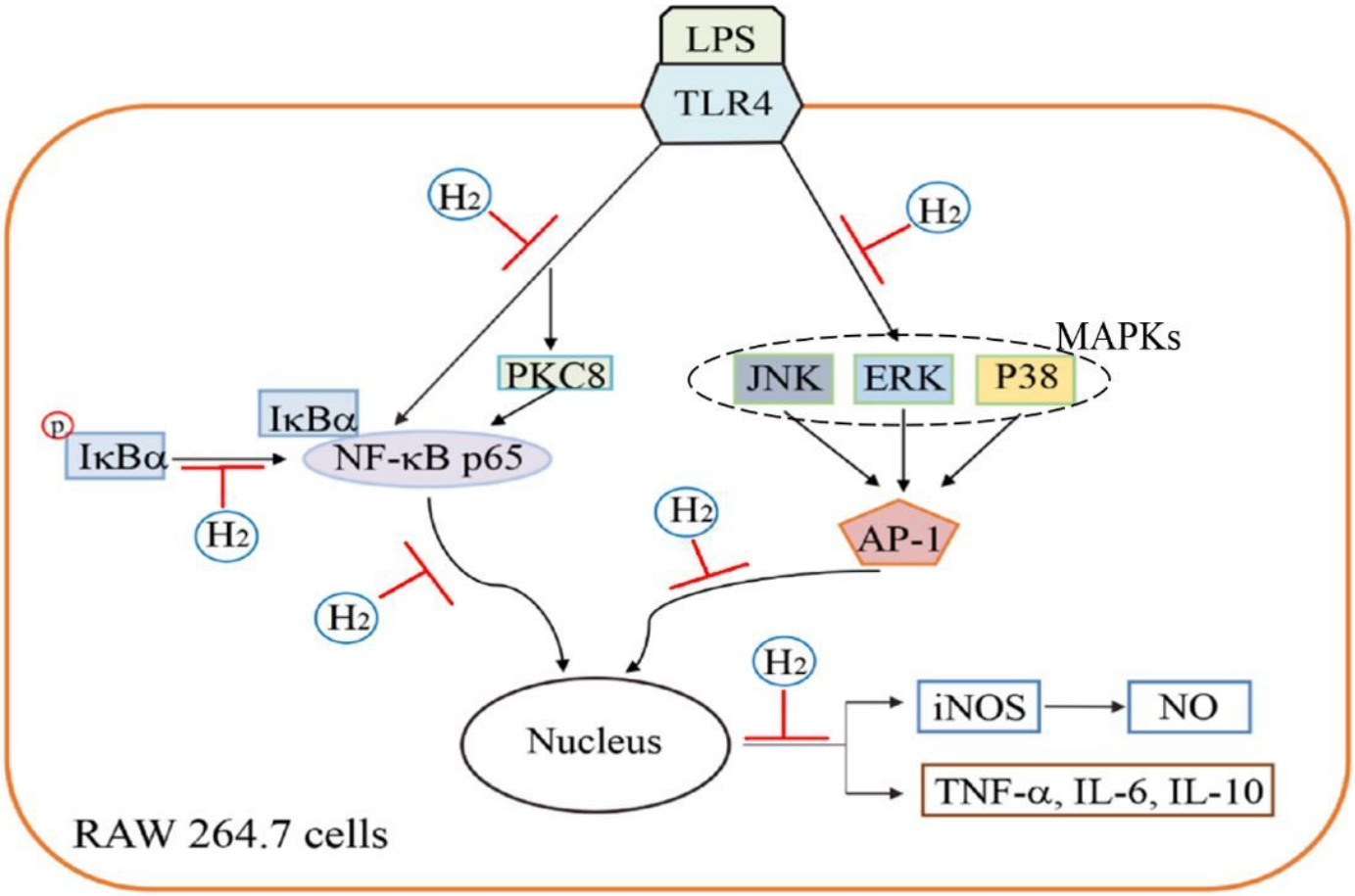

Figure 8

Schematic illustration of the molecular pathways associated with the anti-inflammatory effect of H2 in LPS-stimulated inflammatory reactions.

Supplementary Files

This is a list of supplementary files associated with this preprint. Click to download.

- 5.pdf